

## A REVIEW OF RECENT AIRCRAFT CONCEPTS EMPLOYING SYNERGISTIC PROPULSION-AIRFRAME INTEGRATION

**Julian Bijewitz, Arne Seitz, Mirko Hornung**  
**Bauhaus Luftfahrt e.V., Taufkirchen, Germany**

**Keywords:** *distributed propulsion, propulsion system integration, boundary layer ingestion*

### Abstract

Recognizing the attention currently devoted to the exploration of a more synergistic propulsion system integration, this technical paper provides a review of recently studied aircraft concepts featuring tightly-coupled engine airframe integration solutions. Initially, a comprehensive overview is given regarding the various facets novel integration options such as distributed propulsion architectures may offer with regards to improvements in vehicular efficiency. Thereafter, the challenges associated with strongly integrated propulsion systems are discussed. An array of design solutions currently under investigation by industry and academia are screened, ranging from unmanned to commercial long range applications. A classification scheme is proposed, based upon which an assessment process is described including the evaluation of the system complexity. Several statistical analyses are presented aiming at the derivation of trends and heuristics applicable to distributed propulsion vehicles: starting from the evaluation of the relations between purpose, methods and implementation approaches employed by distributed propulsion concepts, further studies focus on the identification of important characteristics relative to existing transport aircraft. This includes key geometric parameters, system architecture characteristics as well as an assessment of the integrated performance.

### Nomenclature

#### Symbols:

$E$  Energy [Wh]

|              |   |
|--------------|---|
| $e$          | Specific energy [Wh/kg]                       |
| $M_{cr}$     | Mach number at typical cruise [-]             |
| $m$          | Mass [kg]                                     |
| $n$          | Numerical quantity [-]                        |
| $R$          | Range [nm]                                    |
| $\alpha$     | Weighing factor [-]                           |
| $\phi$       | Complexity index [-]                          |
| $\zeta_{en}$ | Energy mass fraction ( $= m_{en}/MTOW$ ) [-]  |
| $\zeta_{oe}$ | Empty mass fraction ( $= OEW/MTOW$ ) [-]      |
| $\zeta_{pl}$ | Payload mass fraction ( $= m_{pl}/MTOW$ ) [-] |
| $\xi$        | System architecture descriptor [-]            |

#### Subscripts:

|      |           |
|------|-----------|
| conc | concept   |
| des  | design    |
| en   | energy    |
| pl   | payload   |
| ref  | reference |

#### Abbreviations:

|      |  |
|------|--|
| A/C  | Aircraft   |
| AFP  | Aft-Fuselage installed Propulsor                         |
| BHL  | Bauhaus Luftfahrt  |
| BLI  | Boundary Layer Ingestion                                 |
| BWB  | Blended Wing Body  |
| CFF  | Cross Flow Fan   |
| CNB  | Commercial Narrowbody                                    |
| CWB  | Commercial Widebody                                      |
| DSP  | Distributed/Synergistic<br>Propulsion system integration |
| DP   | Distributed Propulsion                                   |
| DiPs | Distributed Propulsors                                   |
| DEX  | Distributed Exhaust                                      |
| EPC  | Energy-to-Power Converter                                |
| ESAR | Energy Specific Air Range                                |
| EST  | Energy Storage Type                                      |
| FHV  | Fuel Heating Value                                       |
| GA   | General Aviation   |

|      |   |
|------|---|
| HWB  | Hybrid Wing Body                              |
| MIL  | Military Transport Aircraft                   |
| MTOW | Maximum Takeoff Weight                        |
| NASA | National Aeronautics and Space Administration |
| OEI  | One Engine Inoperative                        |
| OEW  | Operating Empty Weight                        |
| PAV  | Personal Air Vehicle                          |
| PAX  | Passengers                                    |
| PMAD | Power Management and Distribution             |
| PPC  | Power-to-Power Converter                      |
| PPT  | Power-to-Power Transmitter                    |
| PREE | Payload-Range-Energy Efficiency               |
| PTC  | Power-to-Thrust Converter                     |
| STOL | Short Takeoff and Landing                     |
| TaW  | Tube and Wing aircraft                        |
| UAV  | Unmanned Aerial Vehicle                       |
| VTOL | Vertical Takeoff and Landing                  |
| WF   | Wake Filling                                  |

## 1 Introduction

In an effort to narrow down the gap between the incremental enhancement of conventional technology, and the long-term environmental targets espoused by aviation worldwide [1-4], further significant efficiency improvements of the propulsion and power system as well as the airframe are crucial. As engine installation issues tend to become more pronounced with ever decreasing specific thrust levels, and attainable system efficiency gains are expected to flatten out when retaining conventional propulsion system integration, the exploration of novel aircraft morphologies is considered to be a key factor. In this respect, the perspective of introducing a more tightly coupled propulsion-airframe integration has generated much attention throughout the aeronautical community.

The benefits potentially attainable from aircraft designed according to a distributed and synergistic propulsion system integration paradigm are manifold. In particular, the exploitation of thus far untapped system level synergies is of interest when departing from the classic separation of airframe and propulsion system. These effects cover various disciplines

such as aerodynamics, propulsion, structural design and flight controls. For example, the principles of boundary layer ingestion (BLI) and wake filling (WF) have been identified as promising ways of utilizing distributed propulsion systems. By entraining the boundary layer developing on wetted surfaces of the airframe into a propulsion system appropriately designed to compensate the airframe momentum deficit through a momentum increment, a reduction in induced over-velocities and hence propulsive power demand can be attained [5]. Different implementation strategies of BLI have been proposed for transport aircraft ranging from aft-fuselage encircling installations [5-11] and double-bubble configurations [12] to Blended Wing Bodies featuring ingestion of parts of the upper centerbody boundary layer [13-16].

By introducing novel propulsor arrangements, very low specific thrust levels without yielding excessive propulsor diameters may become practical, thereby paving the way towards reduced noise emissions. Further potential to noise reductions may be offered through engine shielding, which, depending on the aircraft configuration, can often be realized more easily than with traditional tube and wing layouts.

Motivated by remarkable advancements in gravimetric specific energy and power of electro-chemical on-board storage equipment and electric machinery, partially or fully electrified power trains are currently under extensive investigation, see e.g. References [17-23]. Apart from the prospect of improved efficiencies of the energy and propulsion system, this allows the decoupling of energy-to-power conversion and power-to-thrust conversion. Such an approach opens up novel ways to synergistically arrange the power and thrust generating devices, and allows for independent control of core engine and propulsor, thereby possibly enhancing the operational behavior of the power plant. As a practical solution, multiple remotely placed propulsors may be arranged such that the aerodynamic characteristics of the aircraft become improved. This involves enhanced high-lift generation but may also refer to beneficial cascade effects due to the feasibility

of smaller sized lifting surfaces [24, 25]. In the field of distributed propulsion, hybrid electric power trains have thus far been considered for small scale unmanned applications to commercial widebody aircraft.

Also, as distributed electric propulsion may be beneficially combined with vertical take-off and landing technology, new possibilities for personal transport and on-demand mobility may become feasible [25-27]. In addition, the arrangement of multiple propulsors may allow for novel flight control options in terms of vectored or differential thrust, thus giving scope to decreasing or even eliminating control surface areas. The influence of propulsors may be used to actively adapt the aero-elastic characteristics of airframe components [28]. Structural weight reductions are often associated with arrangements allowing the omission of classic propulsion installation such as pylons and parts of the nacelle structure. Concurrently to (hybrid-) electric solutions, also power distribution through shaft and gear systems [14-16] as well as pneumatic options [29-31] have been explored.

Apart from the discussed beneficial effects also challenges arise from a more closely-couple engine integration. For BLI applications this typically refers to the distortion of the propulsor inflow field with potentially detrimental effects on fan efficiency and stability, and typically degraded intake pressure ratios as a result of the low-momentum boundary layer flow [5, 6]. Architectures with decentralized or remotely arranged propulsors typically incur additional losses along the transmission chain. For hybrid and fully electric transport aircraft, still further advances in the characteristics of energy storage, distribution and conversion devices are required. Multiple laterally arranged propulsors require careful positioning or dedicated design measures in order to avoid safety issues in case of uncontained engine failures.

The purpose of this paper is to provide a review of aircraft concepts with strongly coupled propulsion airframe integration investigated in the recent timeframe. Based upon technical data taken from literature sources, several analyses will be presented to explore the purpose, mechanisms and implementation strategies

associated with distributed and synergistic propulsion system integration. Moreover, the implications regarding system complexity, geometry and integrated performance will be discussed.

## **2 Overview of Distributed Propulsion Aircraft**

Sehra *et al.* [32] pointed out the benefits of realizing a fully integrated airframe and propulsion system and offered an initial compilation of distributed propulsion (DP) candidate solutions. Kim [33] presented a classification of DP types and discussed selected examples. Gohardani *et al.* gave comprehensive historic overviews of distributed propulsion configurations and related technologies [34]. Additional synopses of possible design solutions and associated technologies can be found in [35-38].

In previous reviews concerned with DP the term “distributed propulsion” was occasionally tied to the number of propulsor units utilized [34]. In the present context, an extended scope is covered. Similar to the characterization given in [33], here, aircraft concepts are considered where in general propulsion-airframe integration is configured such that synergistic benefits are maximized from the outset. Note that this does not necessarily require multiple propulsors but could in principle be afforded by a single one. These concepts will be subsumed under the term “Distributed / Synergistic Propulsion System Integration” (DSP), where DP configurations constitute an important subset.

### **2.1 Data Basis**

With the intent to consider a wide range of possible applications for DSP systems in the analyses following, an extensive survey on DSP design solutions was conducted and essential information was derived primarily from technical publications. In total, 40 concepts were captured and considered to be a sufficiently representative set of sample points of recent DSP activities. The timeframe in which the screened concepts have been

published ranges from 2003 to the first quarter of 2016. One historic concept (Breguet 941) was included as a famous representative of early applications of DSP technology. For the sake of comparison to the trends of a representative array of contemporary in-service transport aircraft, the corresponding key parameters were taken from manufacturer information (primarily airport planning documents). Both turbofan and turboprop powered aircraft were included. Payload and range characteristics were compared at design conditions assuming typical seating arrangements and a specific passenger payload of 100 kg/PAX including luggage, if not otherwise specified in the literature.

The considered DSP concepts were grouped into several categories including:

- Unmanned Aerial Vehicle (UAV)
- Personal Air Vehicle (PAV)
- General Aviation (GA)
- Military Transport Aircraft (MIL)
- Commercial Narrowbody (CNB)
- Commercial Widebody (CWB)

For the classification of PAV concepts the specification given by NASA [26, 27] was adopted. Moreover, the concepts were clustered according to the airframe morphology including “tube and wing” layouts, “blended wing bodies”, “flying cars” offering multi-modal transport and “other”, which is applicable to unconventional layouts such as polyhedral wings or three-surface designs not fitting into the above given categories.

## 2.2 Classification of Distributed Propulsion Concepts

In order to gain additional insight as to what topological options and propulsion system integration approaches have been pursued in the field of DSP, a scheme for the classification of DSP concepts is proposed. Targeting the applicability to a broad range of aspects pertinent to DSP, the scheme separately assesses the *purpose* a certain concept fulfills by using a DSP approach, the *mechanism* (i.e. critical technology aspects) that is used to address that purpose as well as the *implementation approach*. Note that for the first two aspects

multiple selections may be applicable. The criteria for each aspect are presented in Tab. 1.

| Purpose                                  | Mechanism                               | Implementation Approach                            |
|--|---|--|
| - Lift augmentation                      |   |  |
| - Drag reduction                         | - BLI / WF                              |  |
| - Enable V/STOL                          | - Thrust vectoring                      | - Distributed propulsors <sup>b</sup>              |
| - Reduction of external noise            | - Engine shielding                      | - Distributed exhaust                              |
| - Improved system redundancy             | - Powered lift                          | - Cross-flow fan                                   |
| - Improved propulsion system performance | - Very low specific thrust <sup>a</sup> | - Aft-fuselage installed propulsor(s) <sup>c</sup> |
| - Enhanced flight control systems        |   |  |

<sup>a</sup> at acceptable fan diameters

<sup>b</sup> distributed along lifting surfaces

<sup>c</sup> includes e.g. (upper-)surface installed, (semi-) embedded and encircling fan arrangements

**Tab. 1: Distributed Propulsion classification scheme**

“Lift augmentation” includes the increase in maximum lift coefficient enabled e.g. by powered lift technologies such as externally blown flaps. “Drag reduction” refers e.g. to vortex-induced drag via very high aspect ratio wing designs, but also to the elimination of apparent airframe drag through boundary layer ingestion and consecutive wake filling, leading to a reduction in motive power required. VTOL may be realized through thrust vectoring, i.e. tilting of either dedicated lift propulsors, all propulsors or even entire lifting surfaces. External noise reduction can be achieved by embedding engines into the airframe, or by introducing an arrangement of control surfaces and power plants such that noise emissions are shielded to the exterior. “Improved system redundancy” is measured relative to traditional twin-engine layouts. In particular, turbo-electric layouts allow for flexibility between power and thrust producing devices and hence enable strategies where a limited number of core engines drives a large number of propulsors. In case of a core engine failure this allows for multiple propulsors still being available and thus ensures a uniform distribution of the remaining power. In addition, cases were



identified with more than two power generators still operating in the OEI case.

Additional synergy effects may be attainable from “enhanced flight control systems” such as differential thrust modulation for configurations with multiple propulsors, and the avoidance of asymmetric thrust during OEI events, which could result in reduced control surface area.

Possible implementation solutions include distributed propulsors (DiPs) arranged along lifting surfaces. Note that this category includes both ducted and unducted devices and is applicable to cases of multiple discrete engines, or common core/multiple propulsor arrangements with either mechanical or electrical connection. A continuous blowing out of the trailing edge of the wing (distributed exhaust, DEX) to achieve wake filling, thrust vectoring or flap blowing was identified as a further possible candidate. The cross-flow fan (CFF) constitutes a spanwise-installed 2D propulsor with beneficial high-lift capability [39-42], while previously mentioned aft-fuselage installed propulsors (AFP) could be fashioned as upper-surface installed arrangements, (semi)-embedded in the airframe or encircling the fuselage. For transport aircraft this installation is often intended to employ BLI and wake filling. Each of the surveyed DSP concepts was subsequently assessed according to the criteria given in Tab. 1. The results along with key information for each considered concept are included in Tab. 2 (overleaf).

### **3 The Assessment Approach**

This section initially highlights the variety of system architectures applicable to DSP concepts and proceeds to describe the assessment approach used to comparatively evaluate system complexity as well as the integrated performance.

#### **3.1 Definition of System Architecture Classes**

In order to consistently cluster the DSP concepts with respect to their system architectures, a classification scheme was established and applied to the concepts. The scheme targets the generalized treatment of conventional as well as

advanced options including mechanical and pneumatic propulsion distribution as well as hybrid and fully electric propulsion architectures. Thus, the setup is independent of the energy type(s) employed in the aircraft. The chosen approach is based upon a balance between a sufficiently detailed resolution and the intent to only rely on a relatively small amount of information. As a result, the model is applicable to all considered concepts. The chosen approach subdivides each architecture into a set of classes which are restricted to the major system component groups. Aircraft systems requiring in-depth information such as the power management and distribution (PMAD) system are not explicitly resolved and instead represented by a single surrogate element. The system boundaries and interfaces between the classes were tailored to ensure applicability to all energy types and power transmission paradigms considered. The description of the classes is given below:

- **Energy-to-Power Converter (EPC)** refers to the class which includes all systems between the energy storage and the conversion into power. The type of power (e.g. shaft power, electrical power,...) is not specified. It includes batteries, heat-based engines such as gas turbines and piston engines, as well as fuel cells, including the associated fuel system.
- **Power-to-Power Converter (PPC)** is a proxy for all components converting a power from one type into another. Examples include electrical motors, or the reverse principle, i.e. generators.
- **Power-to-Power Transmitter (PPT)** is used to transmit a non-specified type of power. A gearbox constitutes a mechanical PPT, while a PMAD is an example for a PPT related to electric power.
- **Power-to-Thrust Converter (PTC)** comprises components generating net thrust such as propellers or ducted fan and nozzle arrangements.

Based upon the modular arrangement of the classes defined above, a number of generic system architecture types (indices *A* through *K*)

were defined. The identified types range from conventional mechanical layouts to fully electric options covering several cases of electrified power trains. Following Reference [68], the distinction between a serial and parallel

architecture depends on whether the power node between the system constituents is of electrical (serial hybrid) or mechanical (parallel hybrid) nature. Obviously, mixed architecture types are also possible.

| Concept Designation <sup>a</sup> | A/C type | Morphology <sup>b</sup> | $R_{des}$ [nm] | PAX <sup>c</sup> | Sys. arch. index <sup>d</sup> | $n_{EST}$ [-] | $n_{EPC}$ [-] | $n_{PPC}$ [-] | $n_{PPT}$ [-] | $n_{PTC}$ [-] | Refs.   |
|----------------------------------|----------|-------------------------|----------------|------------------|-------------------------------|---------------|---------------|---------------|---------------|---------------|---------|
| LEAPTech                         | GA       | TaW                     | 200            | 4                | <i>H</i>                      | 2             | 2             | 19            | 1             | 18            | [24]    |
| Reynolds <i>et al.</i> (2014)    | CNB      | TaW                     | 3980           | 200              | <i>D</i>                      | 1             | 2             | 10            | 1             | 8             | [28]    |
| Joby S2                          | PAV      | TaW                     | 174            | 2                | <i>K</i>                      | 1             | 1             | 12            | 1             | 12            | [25]    |
| NASA GL-10                       | UAV      | TaW                     | - <sup>e</sup> | n/a              | <i>D</i>                      | 1             | 1             | 11            | 1             | 10            | [43]    |
| NASA/MIT D8.2                    | CNB      | TaW                     | 3000           | 180              | <i>A</i>                      | 1             | 2             | 0             | 0             | 2             | [13,44] |
| ESAero <sup>f</sup> ECO-150      | CNB      | TaW                     | 5500           | 150              | <i>F</i>                      | 2             | 3             | 18            | 1             | 16            | [18]    |
| e-volo VC200                     | PAV      | O                       | ~54            | 2                | <i>H</i>                      | 2             | 2             | 19            | 1             | 18            | [45]    |
| NASA N3-X                        | CWB      | BWB                     | 7500           | 300              | <i>D</i>                      | 1             | 2             | 16            | 1             | 14            | [14,46] |
| SOAR FanWing <sup>g</sup>        | CNB      | O                       | -              | 65               | <i>A</i>                      | 1             | 2             | 0             | 0             | 2             | [47]    |
| Joby Lotus <sup>h</sup>          | PAV      | TaW                     | 700            | 2                | <i>G</i>                      | 2             | 2             | 3             | 1             | 3             | [48]    |
| SAX-40                           | CWB      | BWB                     | 5000           | 215              | <i>B</i>                      | 1             | 3             | 0             | 9             | 9             | [14,49] |
| NASA/MIT H3.2                    | CWB      | BWB                     | 7600           | 354              | <i>B</i>                      | 1             | 2             | 0             | 6             | 4             | [15]    |
| Quantum Systems VRT              | UAV      | TaW                     | 270            | n/a              | <i>K</i>                      | 1             | 1             | 4             | 1             | 4             | [50]    |
| OliverVTOL Hexplane              | CNB      | O                       | 1300           | ~100             | <i>A</i>                      | 1             | 6             | 0             | 0             | 6             | [51]    |
| Boeing SUGAR Freeze <sup>i</sup> | CNB      | TaW                     | 3500           | 154              | <i>E</i>                      | 1             | 2             | 3             | 1             | 3             | [11]    |
| Epstein (2007)                   | MIL      | TaW                     | 1000           | 33               | <i>A</i>                      | 1             | 30            | 0             | 0             | 30            | [52]    |
| NACRE FW2                        | CWB      | BWB                     | 7650           | 750              | <i>A</i>                      | 1             | 3             | 0             | 0             | 3             | [53]    |
| Leifsson <i>et al.</i> (2005)    | CWB      | BWB                     | 7750           | 478              | <i>C</i>                      | 1             | 8             | 0             | 0             | 1             | [54]    |
| Ko <i>et al.</i> (2003)          | CWB      | BWB                     | 7000           | 800              | <i>C</i>                      | 1             | 8             | 0             | 0             | 1             | [31]    |
| Luongo <i>et al.</i> (2009)      | CNB      | TaW                     | -              | 100              | <i>D</i>                      | 1             | 2             | 12            | 1             | 10            | [17]    |
| Gologan <i>et al.</i> (2009)     | CNB      | TaW                     | -              | 50               | <i>B</i>                      | 1             | 2             | 0             | 2             | 4             | [42]    |
| BHL Claire Liner                 | CWB      | O                       | 2000           | 300              | <i>B</i>                      | 1             | 2             | 0             | 6             | 4             | [55]    |
| BHL Propulsive Fuselage          | CWB      | TaW                     | 4800           | 340              | <i>A</i>                      | 1             | 3             | 0             | 0             | 3             | [8]     |
| XTI TriFan 600                   | PAV      | TaW                     | 1500           | 6                | <i>D</i>                      | 1             | 2             | 5             | 1             | 3             | [56]    |
| NASA HyperCommuter               | PAV      | O                       | 174            | 2                | <i>K</i>                      | 1             | 1             | 12            | 1             | 12            | [57,58] |
| Aurora LightningStrike           | UAV      | O                       | -              | n/a              | <i>D</i>                      | 1             | 1             | 25            | 1             | 24            | [59]    |
| NASA STARC-ABL                   | CNB      | TaW                     | 3500           | 154              | <i>E</i>                      | 1             | 2             | 3             | 1             | 3             | [9]     |
| SOAR FanWing <sup>j</sup>        | CNB      | O                       | -              | n/a              | <i>A</i>                      | 1             | 2             | 0             | 0             | 2             | [47]    |
| Joby Lotus <sup>k</sup>          | PAV      | TaW                     | 140            | 2                | <i>K</i>                      | 1             | 1             | 3             | 1             | 3             | [48]    |
| Joby Lotus UAV                   | UAV      | TaW                     | -              | n/a              | <i>G</i>                      | 2             | 2             | 3             | 1             | 3             | [60]    |
| NASA N2B                         | CWB      | BWB                     | 6000           | 0                | <i>B</i>                      | 1             | 3             | 0             | 9             | 9             | [16]    |
| NASA CESTOL BWB                  | CWB      | BWB                     | 3000           | 170              | <i>A</i>                      | 1             | 12            | 0             | 0             | 12            | [62]    |
| Univ. Virginia Sustinere         | CNB      | TaW                     | 500            | 50               | <i>D</i>                      | 1             | 2             | 10            | 1             | 8             | [63]    |
| ESAero <sup>f</sup> ECO-250      | CWB      | TaW                     | 5125           | 250              | <i>F</i>                      | 2             | 3             | 12            | 1             | 10            | [18]    |
| TacticalRobotics Cormorant       | UAV      | FC                      | 162            | n/a              | <i>B</i>                      | 1             | 1             | 0             | 4             | 4             | [63]    |
| UrbanAeronautics X-Hawk          | MIL      | FC                      | -              | 10               | <i>B</i>                      | 1             | 2             | 0             | 7             | 4             | [64]    |
| Airbus Group VoltAir             | CNB      | TaW                     | 900            | 65               | <i>K</i>                      | 1             | 1             | 1             | 1             | 1             | [10]    |
| Pilczer (2003)                   | CWB      | BWB                     | -              | -                | <i>C</i>                      | 1             | 9             | 0             | 0             | 1             | [65]    |
| Airbus Quadcruiser Demo.         | UAV      | O                       | -              | -                | <i>K</i>                      | 1             | 1             | 5             | 1             | 5             | [66]    |
| Breguet 941                      | CNB      | TaW                     | 540            | 57               | <i>B</i>                      | 1             | 4             | 0             | 4             | 4             | [67]    |

<sup>a</sup> if the concept has not been assigned a dedicated designation, a most recent reference is used as a descriptor

<sup>b</sup> key: TaW = tube and wing, BWB = Blended Wing Body, FC = Flying Car, O = other

<sup>c</sup> or seating capacity of PAV and GA aircraft

<sup>d</sup> System Architecture Index, see p. 6 for explanation of acronyms

<sup>e</sup> indicates information not found in literature

<sup>f</sup> Empirical Systems Aerospace

<sup>g</sup> cargo version specified in Reference [46]

<sup>h</sup> hybrid-electric version

<sup>i</sup> "Hybrid BLI" version investigated in Reference [51]

<sup>j</sup> passenger version specified in Reference [46]

<sup>k</sup> fully electric version

**Tab. 2: Synopsis of important characteristics of selected DSP concepts**

Below, the considered system architectures are listed in coarsely arranged order of increasing electrification:

- *A*: Fuel-based mechanic (state-of-the-art layout of in-service transport aircraft).
- *B*: Fuel-based mechanic with mechanical distribution through shaft and gear systems.
- *C*: Fuel-based mechanic with pneumatic distribution. This refers e.g. to concepts where the exhaust gas is ejected through a distributed exhaust nozzle, or tip-turbine driven decentralized fan arrangements.
- *D*: Serial hybrid with a single type of energy supply. This includes “turbo-electric” cases where a fuel based power plant generates shaft power, which is subsequently converted to electrical power through a generator. Following distribution in a PMAD, the power is used to drive electric motor(s) ultimately being coupled to PTCs. This constitutes a purely serial hybrid architecture. Possible residual thrust of the turbo-generator(s) is considered negligible. Note that this architecture also captures scenarios, where a fuel cell is used to generate power for electric motor(s).
- *E*: Serial hybrid with a single type of energy supply, where turbo-generators are mechanically connected to a PTC providing additional net thrust.
- *F*: Serial hybrid with multiple types of energy supply. This includes layouts, where electric motor power is drawn from (turbo-) engine offtake, and e.g. from a battery.
- *G*: Serial hybrid, similar to option *F*, with the addition of (turbo-) engines being mechanically coupled to a PTC providing additional net thrust.
- *H*: Range extender architecture, where a fuel based engine is utilized to recharge a battery.
- *I*: Parallel hybrid, where the power shaft of the PTC is connected both to a fuel-based engine and an electric motor.

- *J*: Serial hybrid, similar to type *F*, but without relying on a combustion engine, but rather e.g. on a combination of battery and a fuel cell.
- *K*: Fully electric, single type of electro-chemical energy supply (e.g. battery, super-capacitor)

Note that the given architectures do not represent the complete combinatorial coverage of theoretically possible scenarios, but rather comprises an array of options that appear to be practically relevant.

### 3.2 Definition of a System Complexity Index

The departure from the well-established morphological setup of contemporary transport aircraft and the addition of advanced technological features typically introduces extra system complexity that needs to be balanced against expected enhancements in vehicular efficiency. As the variety of system architectures considered for DSP concepts was found to be large, a comparative assessment of the complexity of the system architectures was deemed particularly important in the present context. Therefore, this section suggests a way to assess different system architectures by introducing a system complexity index ( $\phi$ ) with intent to serve as a metric for initial comparison between the different concepts. The definition of  $\phi$  is based upon the evaluation of the number of instances the above given classes occur within the entire system architecture of a vehicle. In order to reflect the relative importance of the different classes, specific weighting factors

$$\alpha_i \leq 1.0, \sum_i \alpha_i = 1.0 \quad (1)$$

were applied. These may be tuned based upon expert knowledge or the scope of the investigation. Pursuing the purpose of an initial comparative study, in the present context the factors were intuitively selected identically, in the first instance (Tab. 3).

| Weighting factors ( $\alpha$ ) | Value |
|--------------------------------|-------|
| $\alpha_{EPC}$                 | 0.20  |
| $\alpha_{PPC}$                 | 0.20  |
| $\alpha_{PPT}$                 | 0.20  |
| $\alpha_{PTC}$                 | 0.20  |
| $\alpha_{EST}$                 | 0.20  |

**Tab. 3: Applied weighting factors**

As an initial plausibility check, the values of  $\alpha$  were compared to the mass breakdowns of a conventional and an electric power plant: for a generic high-bypass turbofan the fan including nacelle (corresponds to the PTC) accounts for approximately half of the total propulsion system weight [69], which appears to be in agreement with the relative proportions between  $\alpha_{PTC}$  and  $\alpha_{EPC}$ . Similarly, for an electric short range aircraft conceptually investigated in [23], the mass share of the propulsors was found comparable to the share of the electric motors, thus qualitatively verifying the proportions between  $\alpha_{PTC}$  and  $\alpha_{PPC}$ .

The mathematical representation of the complexity index is given as

$$\phi = \sum_{i=1}^N \alpha_i n_i, \quad N \in \{EPC, \dots, EST\} \quad (2)$$

where  $n_i$  represents the number of instances a class  $i$  occurs within a system architecture. For a conventionally powered, twin-engine reference configuration  $\phi$  results in a value of 1.

Note that depending on the available level of detail or system knowledge further refinements to the model may be possible by increasing the resolution of explicitly evaluated components. While, for example, in the present scope electrical and mechanical power transmission types were weighted identically, different sub-weighting factors could be applied to each paradigm.

For demonstration purposes of the established evaluation method, 4 system architectures were selected. Types *A* (conventional) and *K* (fully electric) were chosen to represent the extrema of the range of architectures, while *B* and *D* reflect intermediate solutions. A schematic representation of the general architectural arrangements is presented in Fig. 1 (overleaf), and Tab. 4 shows characteristics of the cases, the computed complexity index and references

to representative examples found in the literature.

With the chosen values of  $\alpha_i$  the turbo-electric layout was found to have a higher  $\phi$  than the other examples. Compared to cases *B* and *K*, the additional complexity is rooted in the requirement to firstly convert shaft power to electrical power, and afterwards transform it back to electrical power supplying the array of electric motors, which eventually convert power to net thrust.

|                      | System Architecture Index <sup>a</sup> |          |          |          |
|----------------------|--|----------|----------|----------|
|                      | <i>A</i> <sup>b</sup>                  | <i>B</i> | <i>D</i> | <i>K</i> |
| $n_{EPC}$            | 2                                      | 3        | 2        | 1        |
| $n_{PPC}$            | 0                                      | 0        | 16       | 12       |
| $n_{PPT}$            | 0                                      | 9        | 1        | 1        |
| $n_{PTC}$            | 2                                      | 9        | 14       | 12       |
| $n_{EST}$            | 1                                      | 1        | 1        | 1        |
| $\phi$               | 1.0                                    | 4.4      | 6.8      | 5.4      |
| Exemplary References | In-service commercial transports       | [14]     | [13]     | [57]     |

<sup>a</sup> see list on pp. 6

<sup>b</sup> Twin-engine reference aircraft

**Tab. 4: Exemplified evaluation of possible system architectures and computed system complexity index**

Pursuing the purpose of describing commonalities and differences intrinsic to the considered system architecture options, relative descriptors are proposed herein. These include the ratio of the number of power-to-thrust converters to energy-to-power converters,

$$\xi_1 = \frac{n_{PTC}}{n_{EPC}} \quad (3)$$

and similarly, based upon  $n_{PPC}$ :

$$\xi_2 = \frac{n_{PPC}}{n_{PTC}} \quad (4)$$

Now, heuristics specific to each considered architecture type may be constructed serving the purpose of establishing relations between the different  $n_i$ . For example, for type *D* the number of PPCs (generators and electric motors) will always be equal to the sum of the number of EPCs (e.g. turboshaft engines) and PTCs (e.g. propellers), see also Tab. 4. Hence, for type *D* this boundary condition can be algebraically formulated as:

$$n_{EPC} + n_{PTC} = n_{PPC} \quad (5)$$



This relation can be conveniently expressed in terms of relative metrics using eq. (3) and (4)

$$\xi_{2,D} = \frac{1 + \xi_1}{\xi_1} \quad (6)$$

and thus gives an indication of the dependency between  $\xi_2$  and  $\xi_1$ .

For some of the remaining types similar conditions as stated in eq. 6 can be fashioned producing the expressions given in Tab. 5.

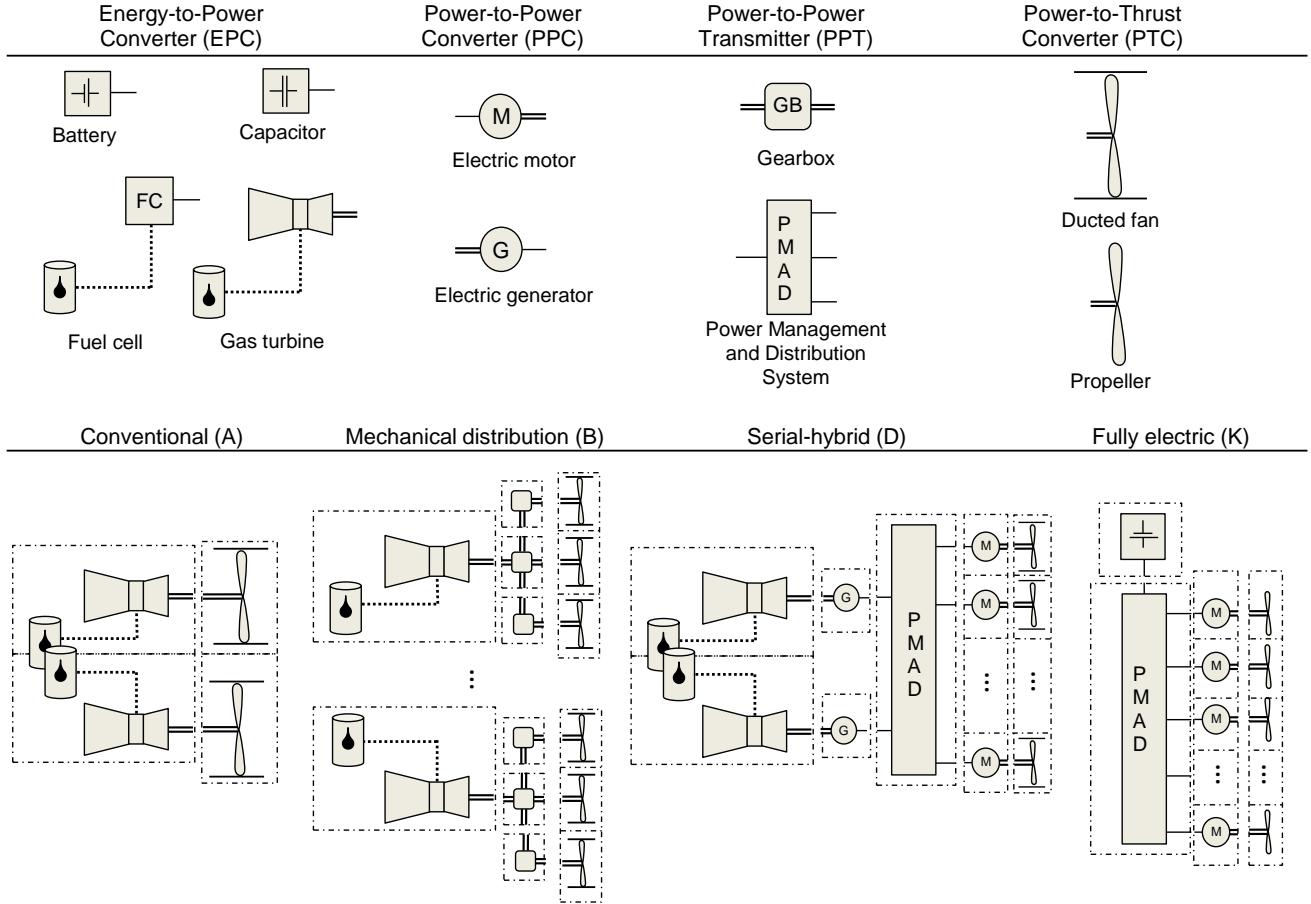


**Fig. 1: Overview of typical components used in system architecture classes (upper part), exemplified arrangements of possible system architectures (lower part)**

| Index     | Boundary Condition                               | Transformed Boundary Condition $\xi_2 = f(\xi_1, n_{EPC})$              | Equation |
|-----------|--|---|----------|
| A,        | $n_{PPC} = 0$                                    | $\xi_{1,A} = 1, \xi_{2,A} = 0$  |          |
| B,C       | $n_{PPC} = 0$                                    | $\xi_{2,B,C} = 0$   |          |
| D         | $n_{EPC} + n_{PTC} = n_{PPC}$                    | $\xi_{2,D} = \frac{1 + \xi_1}{\xi_1}$                                   | (6)      |
| F         | $n_{EPC} - 1 + n_{PTC} = n_{PPC}$                | $\xi_{2,F} = \frac{(1 + \xi_1) \cdot n_{EPC} - 1}{\xi_1 \cdot n_{EPC}}$ | (7)      |
| H         | $n_{EPC} - 1 + n_{PTC} = n_{PPC}, n_{EPC} = 2^a$ | $\xi_{2,H} = \frac{1 + \xi_1 \cdot n_{EPC}}{\xi_1 \cdot n_{EPC}}$       | (8)      |
| E,G, I, J | $n_{EPC} = n_{PTC} + 1, n_{PPC} = n_{PTC}$       | $\xi_{2,E,G,I,J} = 1$   |          |
| K         | $n_{PPC} = n_{PTC}$                              | $\xi_{2,K} = 1$   |          |

<sup>a</sup> this is considered the only practical case

**Tab. 5: Overview of system architecture-specific heuristics**

### 3.3 Metrics for Integrated Performance Assessment

In order to compare and contrast the characteristics of the DSP concepts to the trends of contemporary transport aircraft, the typical weight fractions with respect to MTOW were derived from the data retrieved from the literature. This includes the OEW fraction,  $\zeta_{oe}$ , and the payload fraction,  $\zeta_{pl}$ . For capturing also (hybrid-) electric architectures, the classic fuel fraction was adapted to yield the energy mass fraction,  $\zeta_{en}$ , now comprising the combined mass of the energy constituents stored onboard the aircraft required to perform the design mission including reserves. For traditional fuel based aircraft this refers to the design fuel mass including reserves, while for electric concepts the battery mass is considered instead.

For the assessment of the integrated performance of the DSP concepts, it is useful to employ an appropriate efficiency metric covering both the characteristics of conventionally powered and electric as well as hybrid energy concepts. In the present context, the Payload Fuel Efficiency given by Torenbeek [70] was chosen and suitably generalized, yielding the Payload Range Energy Efficiency,

$$PREE = \frac{m_{pl,des} \cdot R_{des}}{E_{des}} \quad (9)$$

in units of [kg·nm/kWh], where  $m_{PL,des}$  represents the design payload carried over the design mission distance  $R_{des}$  while consuming the energy  $E_{des}$ . Given that in eq. (9) the nominator refers to the income potential, while the denominator is correlated to a large proportion of the operating expenses, PREE can be interpreted as an efficiency of the transport system [70]. For classic fuel based aircraft,  $E_{des}$  and the fuel mass are coupled through the Fuel Heating Value (FHV  $\approx 42.8$  MJ/kg for Jet-A fuel), while for battery-based concepts the knowledge of the gravimetric specific energy of the battery is required to determine  $E_{des}$  from  $m_{en}$ . In case of hybrid energy storage, the sum of fuel and battery based energy constituents needs to be considered. For conventional or fully electric aircraft, PREE can be correlated to the

payload-to-energy mass fraction,  $\zeta_{pl}/\zeta_{en}$ . Recognizing

$$\frac{m_{pl}}{m_{en}} = \frac{m_{pl}}{MTOW} \cdot \frac{MTOW}{m_{en}} \quad (10)$$

eq. (9) can be rearranged as:

$$\frac{m_{PL}}{m_{en}} = \frac{\zeta_{pl}}{\zeta_{en}} = e \cdot \frac{PREE}{R} \quad (11)$$

where  $e$  denotes the specific energy of the battery for fully electric aircraft, or the FHV for conventional applications, respectively.

## 4 Analysis Results and Discussion

Following the discussion of the chronological evolution of DSP concepts, the relations between purpose, method and mechanism will be explored. Apart from the evaluation of system complexity associated with DSP, this section is dedicated to the evaluation of important aircraft parameters and the integrated performance.

### 4.1 Evolution of Distributed Propulsion

Fig. 2 (overleaf) presents the chronological evolution of the concepts included in Tab. 2. On the abscissa the timeframe in which each concept was or has been investigated is displayed, while the ordinate shows the design range. For simplification, the timeframe was aligned with the interval in which scientific publications have been published. The marker symbols indicate the different aircraft types and the colors refer to the system architecture type. For readability purposes the transmission architectures were clustered into fuel-based, mechanic transmissions (index A through C), hybrid-electric types (D through J) and fully electric types (K).

The increasing density of sample points towards the right end of the chart illustrates the growing interest devoted to DSP. With regards to the energy storage types employed, it is visible that electric DSP aircraft have only emerged in the recent timeframe and are currently primarily considered for GA, PAV and UAV applications with limited design ranges. Only one projected concept was found showing a design range

compatible with the typical regional aircraft segment. In contrast to that, hybrid-electric concepts show a much larger bandwidth in range up to 7500 nm, which was found comparable to the values immanent to mechanically powered concepts. Purely fuel-based concepts are distributed across the entire timeframe considered and were found (apart from one outlier) to be exclusively associated with CWB, CNB and MIL aircraft types. It can be concluded that for small aircraft types clearly a trend to employ fully electric propulsion is emerging, while in order to fulfill the mission requirements of large commercial aircraft these DSP concepts primarily rely on a non-battery based energy source as realized e.g. with turbo-electric layouts. Here, a gradual departure from the purely mechanical drive train is noticeable. In summary, the combination of DSP and electric drive technology seems to be a particularly attractive field for advanced studies.

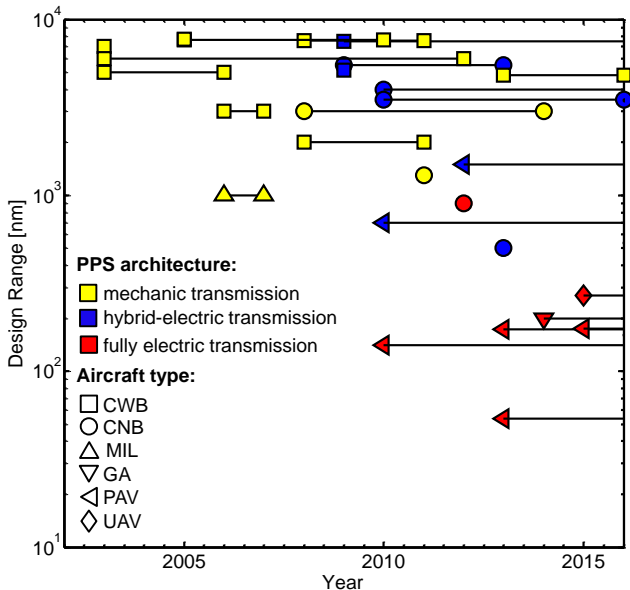


**Fig. 2: Evolution of DSP research activities over time**

#### 4.2 Purpose, Mechanism and Implementation of Distributed Propulsion

The available data was analyzed with respect to the DSP classification scheme given in Section 2.1. Aspects of the results are elucidated in Fig. 3, which displays the number of instances in which an implementation approach was employed in one of the defined aircraft types.

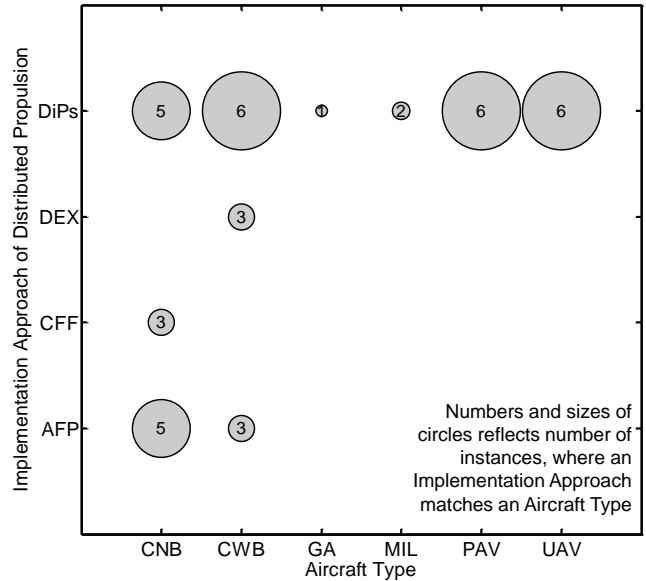
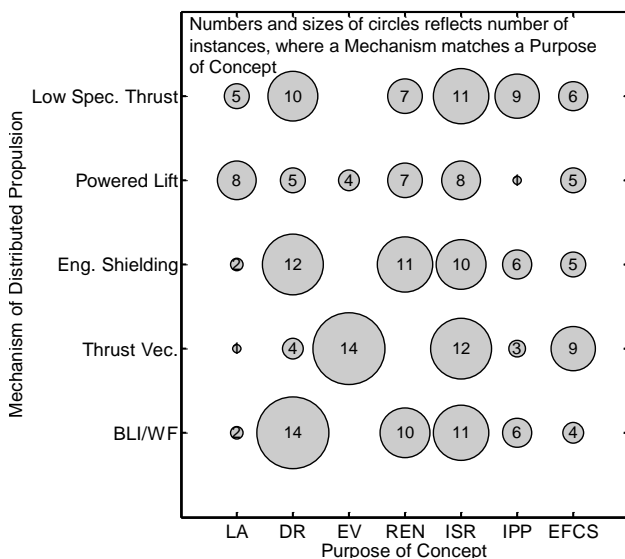


**Fig. 3: Implementation approach and aircraft types**

It is apparent that DiPs are used for the entire spectrum of aircraft types considered. AFPs are found to be primarily applied in the commercial aircraft segment. Moreover, GA, MIL, PAV and UAV aircraft are found to be exclusively designed using a distribution of propulsors. While for PAV and UAV this is frequently motivated through VTOL requirements necessitating multiple propulsors, the inexistence of combinations of GA and MIL with other than DiPs may be attributed to the current limitation of the dataset. For CNB and CWB aircraft, aft-installed propulsors are often associated with BLI. This appears to be less relevant for smaller applications such as GA, PAV and UAV due to much thinner boundary layer flows. However, the fact that there are applications with aft-fuselage propulsor existing in that segment [71-74] indicates other advantages stemming from such a propulsion integration, e.g. the fuselage being not immersed in the propeller wash. In a general sense it can be concluded that only a fraction of the theoretically possible combinations have been actively considered yet.

Some combinations might lack the practical feasibility such as the application of DEX to PAV and UAV as for these types most frequently electrical power trains are used. On the other hand, the installation of a CFF to GA, MIL, PAV or UAV types may constitute promising candidates for further studies, e.g.

due to the potentially superior high-lift capability attainable from the CFF.



Abscissa labels: LA = lift augmentation, DR = drag reduction, EV = enable V/STOL, REN = Reduction of external noise, ISR = improved system redundancy, IPP = improved propulsion system performance, EFCS = enhanced flight control systems

**Fig. 4: Mechanism / purpose of distributed propulsion**

Additional insight is offered through Fig. 4, which, similarly as Fig. 3, indicates the instances in which a mechanism of DSP is employed to address a certain purpose of DSP. Intuitively, large accumulations occur for thrust vectoring being applied to realize VTOL. The quantitative superiority of thrust vectoring relative to powered lift technology with regards to the realization of V/STOL indicates the emphasis currently being placed on such propulsion integration options. This may be attributed to the advent of hybrid electric distributed architectures, where a combination with vertical takeoff capability seems to be particularly beneficial. Also, much emphasis is being placed on synergistic propulsion system integration with BLI and wake filling. Technically feasible arrangements with low specific thrust are associated with either mechanical distribution or turbo-electric layouts with remotely driven propulsors. As an implicit result, the system redundancy often becomes improved. Judging from the considerable level of employed combinations, the study demonstrates the high degree of inter-connections between the technologies, and the synergistic potential offered by designing flight

vehicles according to the DSP paradigm. For example, boundary layer ingesting fans may be installed in an airframe-embedded fashion, thus, in addition to ultimately reducing the propulsive power demand, also effectively shielding engine noise to the external. In addition, provided the array of propulsors is arranged appropriately, novel ways of flight control augmentation may be possible, thereby decreasing the required control surface area and hence saving weight and wetted area.

To conclude, the figure reflects the extensive research effort currently being expended to improve overall vehicular efficiency, but also to decrease noise and realize new ways of personal transportation, for which STOL or even VTOL seems to be an important aspect.

### 4.3 Distribution of the Number of Propulsors

After having examined the integration options available for DSP this study focusses on the evaluation of the numerical quantity of power-to-thrust converters ( $n_{PTC}$ ) used in DSP aircraft. Fig. 5 shows the distribution of the number of concepts employing a specific  $n_{PTC}$ . A color code is used to visualize the share of propulsor options that are employed with the analyzed concepts. In addition, the relative cumulative distribution is given on the secondary ordinate. The spectrum of  $n_{PTC}$  ranges from 1 to 30 and both odd and even numbers are used. The highest number of concepts was found to be associated with  $n_{PTC} = 3$ . From the distribution of  $n_{Conc}$  it can be followed that a high share of concepts features a rather low number of EPCs. Specifically, 55% of all concepts have an  $n_{PTC}$  of up to and including 4. All propulsor types are represented within this bandwidth. Concepts with  $n_{PTC} > 18$  appear to be rare, only two samples were found. This is an indication that a very high number of EPCs is only justifiable if certain unconventional aspects are addressed such as maximization of synergistic aeropropulsion interaction and very high redundancy requirements combined with VTOL capability. In essence, synergistic propulsion airframe integration does not necessarily rely on a high number of propulsors.



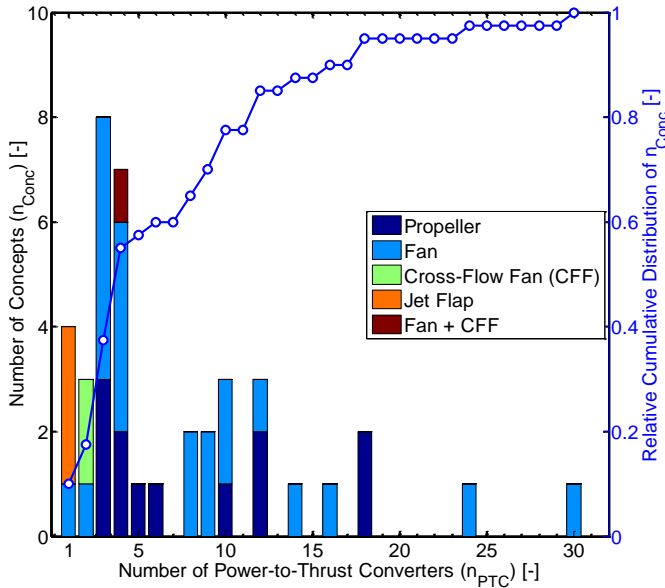
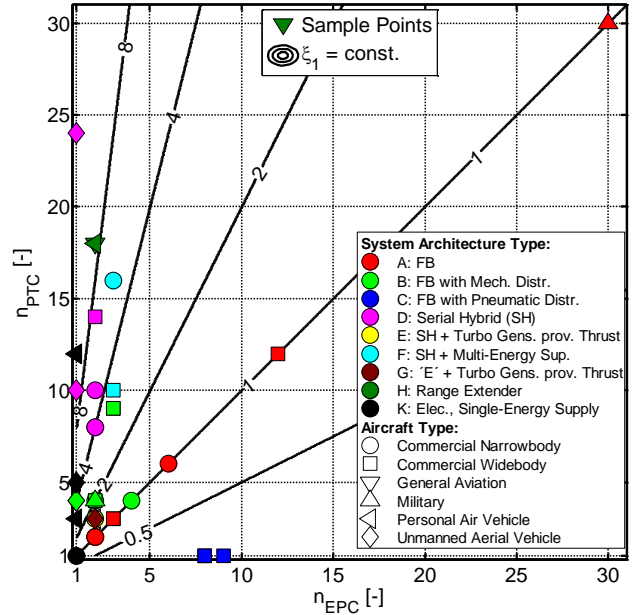


Fig. 5: Distribution of power-to-thrust converters

#### 4.4 Evaluation of the System Complexity Index

Prior to discussing the evaluation of the DSP complexity index, Fig. 6 presents contour lines of the relative descriptor  $\xi_1$  as a function of the absolute numbers of  $n_{PTC}$  and  $n_{EPC}$ . The considered concepts are represented through their respective data points. As can be gleaned from the chart and from inspection of Tab. 5, for classic fuel-based power plants  $\xi_1$  becomes unity reflecting the direct connection between e.g. a turboshaft engine and the propulsor. The majority of concepts are found in the upper triangle ( $\xi_1 \geq 1$ ). This is conceivable since although the installation of a higher number of EPCs than PTCs might be feasible in special cases,  $\xi_1 < 1$  generally appears to lack practical relevance. The two exceptions at  $n_{PTC} = 1$  refer to concepts featuring distributed exhausts, i.e. a continuous jet out of the trailing edge. Apart from the outlier at  $n_{EPC} = n_{PTC} = 30$ , concepts of type *D* feature the highest numbers of PTCs. The increased flexibility enabled through the decoupling of EPC and PTC allows for high numbers of propulsors driven by a small number of core engines. In fact, for type *D*  $n_{EPC}$  was found solely 1 or 2, while the corresponding  $n_{PTC}$  spans a range of 8 to 24 and accordingly, large values of  $\xi_1$  are obtained.



Abbreviations in legend: FB = fuel-based propulsion system, SH = serial hybrid

Fig. 6: Number of power-to-thrust converters vs energy-to-power converters

Fig. 7 (overleaf) provides additional insight with regards to the inter-play of  $\xi_1$  and  $\xi_2$  by showing the evaluation of the analytical relations given in Tab. 5. Apparently, the marker points corresponding to the concepts are aligned with the trending behavior of the identified heuristics pertinent to the system architecture employed in each of the concepts, thus verifying the derived relations. For the conventional power plant, the lines collapse into one single point ( $\xi_1 = 1$ ,  $\xi_2 = 0$ ). Fully electric propulsion systems as well as types *E*, *G*, *I* and *J* feature parallelism to the abscissa ( $\xi_2 = 1$ ,  $\xi_1 > 0$ ). For a given number of EPC and PTC ( $\xi_1 = \text{const.}$ ) increasing values of  $\xi_2$  indicate a growth in power conversion required and therefore, the contour for e.g.  $\xi_{2,D}$  features high values of  $\xi_2$ . In addition,  $\xi_1$  may be interpreted as a measure of the degree of decoupling between EPC and PTC. While, as discussed above, conventional layouts adhere to  $\xi_1 = 1$ , turbo-electric configurations feature a decoupling between the turbo-generator and the thrust producing devices (irrespective of the energy types used along the power train) and hence yield  $\xi_1$  values greater than 1. For example, mechanically distributed options have zero conversion and only moderate degrees of decoupling. On the other hand, architectures

with electrification rely on conversion ( $\xi_2 \geq 1$ ) and exhibit the full range of values for  $\xi_1$ . Due to reasons of physical feasibility, no sample points are found within the interval  $\xi_2 = ]0; 1[$ .

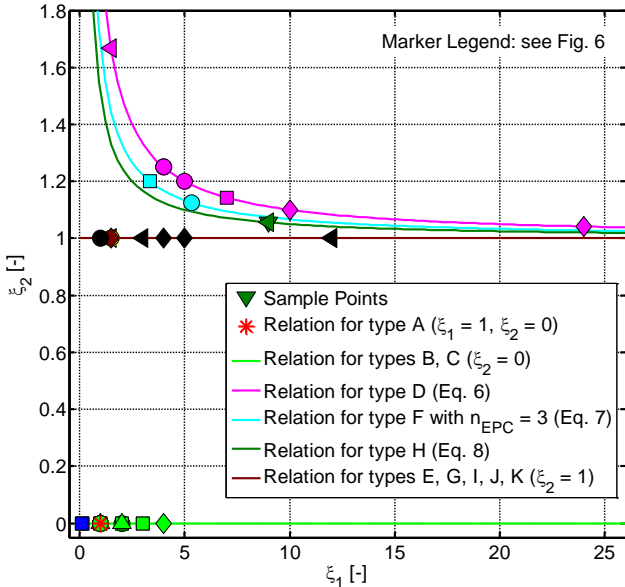


Fig. 7: Heuristics for relative descriptors  $\xi_1$  and  $\xi_2$

In Fig. 8 the evaluation of the relative system complexity index is presented for each system architecture type. The color code refers to the aircraft type while the markers indicate the morphology. Parity in  $\phi$  with the twin-engine reference aircraft is found only for a concept employing a small number of turbofan engines, two representatives of the CFF, and a concept with a single electrically driven ducted fan. Hence, it can be argued that for most concepts an increased complexity is traded against improvements in overall vehicular efficiency or other concept-intrinsic advantages. It is noticeable that no architecture is exclusively used in a specific aircraft type, but different architectural options seem to be employed. Also, no dependency between aircraft size and  $\phi$  was identified. For CNB transports the full range of degrees of hybridization is used, however, the majority of concepts is found to rely on conventional or hybrid architectures. All of the analyzed PAVs feature elements of electrification. It is recognized that for the vast majority of concepts (95%)  $\phi$  does not exceed 9, and 60% have  $\phi$  smaller than 3, signifying the effort expended to minimize system complexity.

No relation was found between the (projected) entry-into-service year and the complexity index. Interestingly, the highest value of  $\phi(12.2)$  is associated with a concept featuring multiple conventional gas turbines. However, this STOL military cargo transport with an array of 30 turbofan engines generating powered lift is considered to be an outlier, where the high level of complexity seems to be accepted to realize very aggressive field performance requirements. Under this premise a value of  $\phi = 11$  appears to be a practical upper limit for currently investigated concepts.

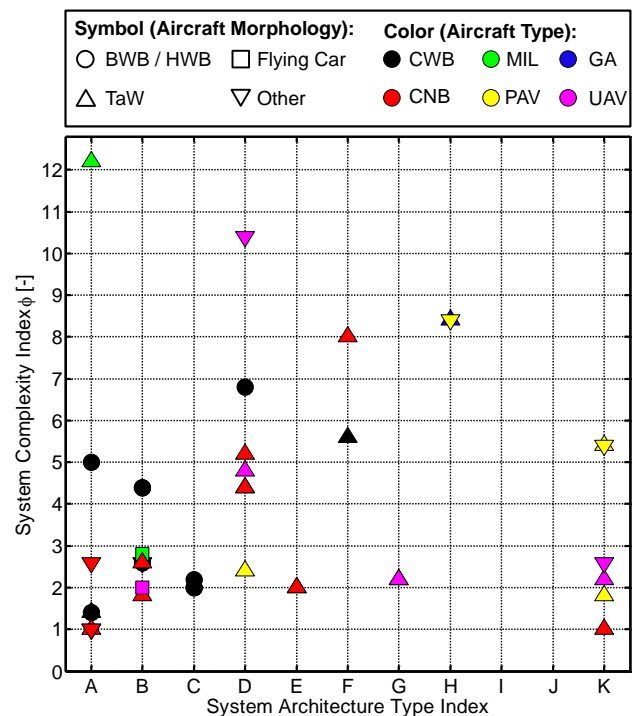


Fig. 8: Evaluation of System Complexity Index

For mechanical distribution options (B), relatively moderate values of  $\phi$  are obtained reflecting the lack of power conversions required. In summary, there is an approximately equal split between concepts with (55%) and without (45%) electrification. No representatives of parallel-hybrid system architectures (I, J) were found during the literature research connected to this paper. Apparently, this hybridization strategy, where extensive research effort has been expended when it concerns conventional, non-distributive configurations (see e.g. References [75-78]), is currently not in the prime research focus in the context of DSP.

Concluding, it has to be noted that apart from its system architecture the overall complexity of the vehicle is also strongly influenced by the airframe morphology itself.

#### 4.5 Analysis of Aircraft Key Parameters

Fig. 9 presents the trending behavior of the wing span ( $b$ ) as a function of MTOW. The color code corresponds to the aircraft types. The well-defined relation between  $b$  and MTOW across several magnitudes of MTOWs and aircraft types is illustrated through the displayed non-linear regression curve satisfying a power-based functional approach. Most sample points reside within a  $\pm 10\%$  confidence interval. Two outliers towards larger values for  $b$  are encountered in the CNB domain corresponding to strut-braced wing configurations indicating the feasibility to apply larger wing spans than exhibited by the general trend.

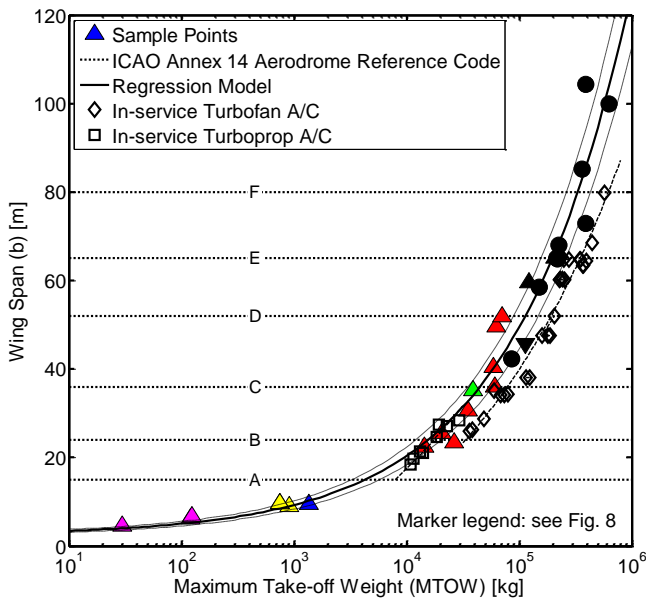


**Fig. 9: Trends of wing span**

For comparison, the figure is supplemented with the respective trends for conventional (turbofan and turboprop powered) aircraft, which were derived using the same functional approach as for the DSP concepts. An offset between the trends for DSP and conventional turbofans is visible reflecting the general trend of advanced concepts to apply larger wing aspect ratios to generate additional benefits from reduced induced drag. The figure also includes the span limitations according to ICAO Annex 14 [79] as

solid lines. Apparently, some concepts have been sized to max out on the span constraint applicable to their respective aerodrome reference code. A few BWB concepts even feature wing spans in excess of all contemporary airport compatibility standards. Fig. 10 displays the typical design cruise Mach number,  $M_{cr}$ , used by the DSP concepts.

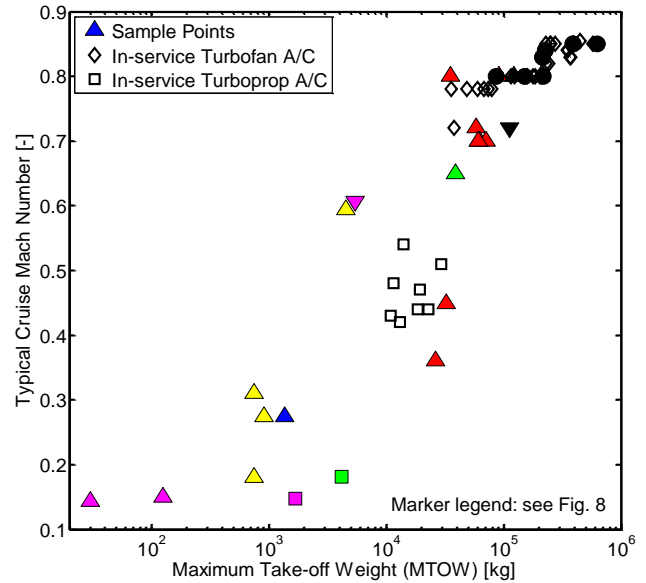


**Fig. 10: Trend of typical cruise Mach number**

Again, for a set of in-service aircraft the corresponding values were derived from manufacturer information and included in the figure. It is visible that for long range applications  $M_{cr}$  is mostly within the domain of conventional aircraft. For CNBs, an agglomeration of concepts is found, which are sized for significantly slower cruise speeds than typically used for conventional turbofan powered aircraft. For some of the concepts this is motivated by the fact that a slower cruise speed and the resulting smaller required wing sweep may be synergistically combined with other annexed technologies such as natural laminar flow [15, 10]. This generates additional fuel efficiency advantages over the benefits attainable from the basic DSP aircraft configuration itself. However, the corresponding penalty in aircraft productivity needs to be recovered e.g. through dedicated operational measures such as improved turn-around times. Also, in addition to mitigated compressibility drag resulting from slower

cruise speeds, the feasibility of decreased wing sweeps is typically associated with reductions in wing structural weight, which constitutes an important portion of the aircraft OEW. This also applies to an electric aircraft, which is sized for a Mach number at the lower end of typical regional applications. As discussed in [80] this is plausible since for electrically powered aircraft the optimum energy-specific air range (ESAR) is typically achieved with a cruise flight technique corresponding to lower Mach numbers compared to similar conventionally powered aircraft. Here, the key influence is related to the shortfall of core engine ram pre-compression for the electric power plant compared to the gas turbine. For turbofan power plants the resulting increase in core efficiency contributes to the improvement of overall propulsion system efficiency with Mach number, while for the electric aircraft the trades between transonic drag rise and power plant efficiency tend to shift the optimum of ESAR to lower Mach numbers.

For UAV and PAV a large spread in  $M_{cr}$  is apparent, reflecting the large variety of mission roles and design paradigms associated with these aircraft types. The fact that Flying Car morphologies operate at low speeds is understandable considering that the configuration must allow for multi-modal capability.

#### 4.6 Survey of Weight Fraction Trends

The weight fractions described in Section 2.1 are presented in Fig. 11 along with the

corresponding trends of contemporary transport aircraft, for which regression curves are shown. For conventional aircraft, the classic trends of decreasing payload and empty weight fractions, as well as increasing energy weight fractions against MTOW are visible [81-83], although for turboprop aircraft the trends of  $\zeta_{en}$  and  $\zeta_{pl}$  were found less distinct than for turbofan powered aircraft. Family members typically featuring commonality in the design of lifting surfaces and systems are connected through dashed lines. For long range aircraft the energy fraction becomes a significant weight share and approaches 50% of the MTOW. While for conventional, in particular, turbofan aircraft most sample points reside within a relatively well defined corridor around the shown regression functions, the DSP concepts tend to deviate from the indicated trend curves.

This may be rooted in the general characteristic that DSP concepts often employ differences in the morphological setup, mission requirements or energy type relative to traditional transports and hence increased scatter is induced to the data. Inspection of Chart II in Fig. 11 reveals the technological advances associated with DSP concepts. Hence, most CNB and CWB configurations feature  $\zeta_{en}$  smaller than the general trend of conventional aircraft, thereby partly triggering increases in  $\zeta_{oe}$ . In particular, BWB layouts consistently feature an offset to lower  $\zeta_{en}$  values rooted primarily in the enhanced aerodynamic efficiency expected from the BWB design. The high payload capacity of BWBs is also visible in Chart III.

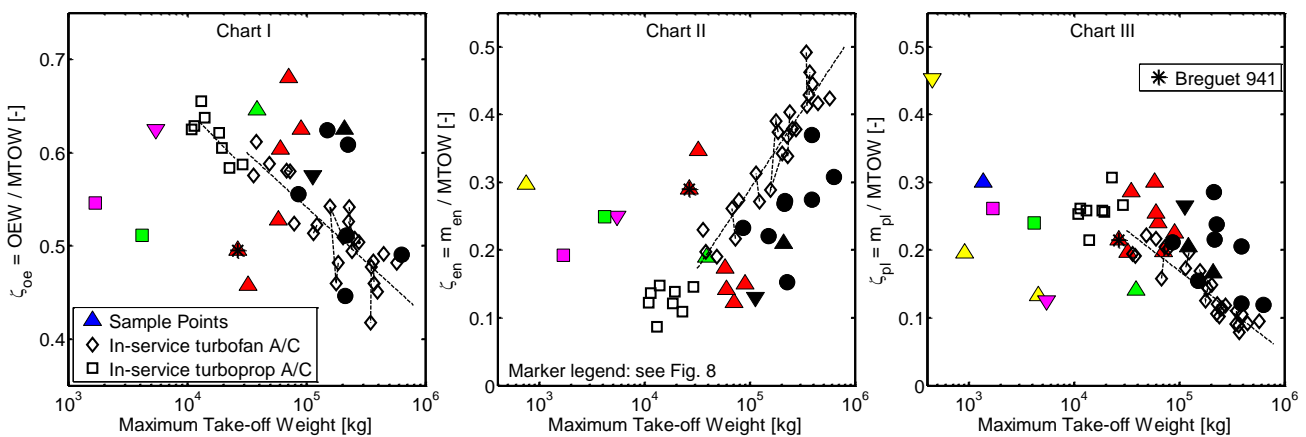


Fig. 11: Fractions of operating empty, energy and payload weight



On the other hand, no clear conclusion can be established regarding the empty weight fraction of BWB relative to those of tube and wing designs [70]. Two outliers in  $\zeta_{en}$  within the CNB domain are encountered. These are related to a historical STOL aircraft (Breguet 941) and a fully electric regional aircraft concept with an understandably large battery mass fraction. PAV and UAV concepts are found off the trend. Examination of Chart I shows that some DSP concepts feature significantly lower OEW fractions than typical for conventional designs. For the two above highlighted concepts in the CNB domain, this is due to unusually high energy mass fractions. For the Flying Car concepts, this may result from the combined effects of a relatively low cruise efficiency (cf. also Chart II) and/or extensive use of advanced materials and manufacturing techniques.

#### 4.7 Comparative Assessment of Integrated Performance

In Fig. 12, the payload-range-energy efficiency PREE is presented as a function of design range. The figure is supplemented with iso-contours of the ratio of payload-to-energy mass fraction,  $\zeta_{pl}/\zeta_{en}$ . For conventional turbofan powered aircraft, a concave trend can be observed resulting from counteracting effects [70]: long range aircraft tend to be penalized through the high fuel load necessary to fulfill the demanding mission requirements leading to a high MTOW and decreasing payload-to-energy mass fractions. For short to medium range aircraft, the fuel fraction used during climb and descent constitutes a substantial share of the block fuel, thus yielding decreased values of PREE. Based upon the analyzed data for conventional turbofan powered aircraft, a weak maximum can be identified around 4000 nm range with corresponding values of  $\zeta_{pl}/\zeta_{en} \approx 0.75$ . For turboprop aircraft higher efficiencies are obtained at similar ranges compared to turbofan powered aircraft reflecting the superior propulsion system efficiency associated with turbo-propeller engines operating at moderate airspeeds. For DSP concepts, the amount of

sample points is insufficient to derive similar trending behaviors.

It is visible in Fig. 12 that technological advances are echoed in increased values of PREE. A distinct cluster of DSP concepts is found for CNB tube and wing aircraft between 3000 and 4000 nm range.

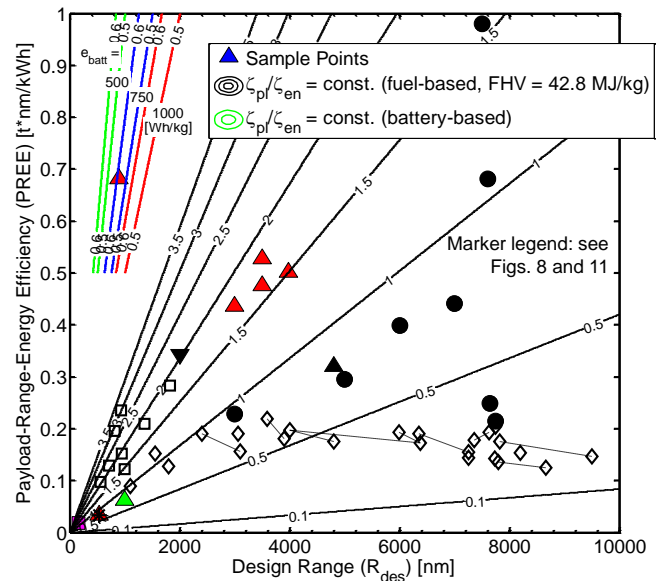


**Fig. 12: PREE as a function of design range**

As noted before, the synergistic combination of aerodynamic improvements, weight reduction technologies and power plant efficiency enhancements enabled through more tightly-coupled propulsion airframe integration allows for substantial improvements in PREE and accordingly increased values of  $\zeta_{pl}/\zeta_{en}$ . Some BWB applications yield particularly high PREE values caused by the high transport capacity enabled by the efficient utilization of volume. A number of concepts feature inferior PREE values compared to in-service aircraft. This may be partly attributed to the special purpose these concepts have been sized for such as superior robustness, extremely high thrust-to-weight ratios etc., thus tolerating deficits in PREE, and, the historic technology level of the Breguet 941. It can be argued that the high energy efficiency of the electric transport aircraft is propagated into high PREE values, however at inferior payload to energy fractions compared to fuel-based aircraft of similar mission role.

In general, the data required to derive PREE proved difficult to find for electric concepts. In the present analysis only for one concept the required parameters were obtainable from the public domain. However, judging from the recent momentum associated with research regarding electrified power trains for airborne applications, increased availability can be expected in the near future.

## 5 Conclusions

Owing to the high level of interest distributed propulsion currently attracts within the aeronautical community, this paper provided a review of distributed propulsion aircraft concepts being or having been investigated within the recent timeframe. The set of design solutions identified includes configurations ranging from unmanned vehicles to long range blended wing body layouts. Considering the advances currently experienced in the field of electro-chemical storage, distribution and power conversion technology, a strong focus on partially and fully electrified power trains was recognized. While projected fully electric aircraft associated with distributed propulsion are currently limited to the regional aircraft segment, hybrid electric configurations were found up to design ranges corresponding to contemporary long range aircraft. Here, the prospect of remotely arranged propulsors driven by a centralized power plant has been intensively studied in multiple projects. Apart from significant enhancements in vehicular efficiency exhibited by more tightly-coupled engine-airframe integration, such configurations also open up new perspectives for personal transport exploiting the principles of vertical takeoff and landing. Based upon an algebraic formulation for a complexity metric, the system complexity of various concepts was analyzed. It should be noted that the presented analysis results rely on the screened data publically available. In future work, a systematic, scenario-based variation of the weighting factors within the complexity metric could be used to assess the robustness of the introduced method. In summary, it was concluded that for most concepts increased system complexity relative

to in-service twin engine aircraft is traded against higher overall vehicular efficiencies. In terms of transport capability per unit energy consumed, clear enhancements in efficiency were identified for most concepts.

In follow-on work the studies presented in this paper will be complemented with additional parameters not explicitly considered yet. Moreover, taking into account additional concepts could increase the density of sample points and hence the statistical significance of the analyses.

## References

- [1] European Commission. "Flightpath 2050: Europe's Vision for Aviation", Report of the High Level Group on Aviation Research, Publications Office of the European Union, Luxembourg, 2011
- [2] Advisory Council for Aviation Research and Innovation in Europe. "Strategic Research and Innovation Agenda", Brussels, 2012
- [3] National Aeronautics and Space Administration (NASA). "Advanced Concept Studies for Subsonic and Supersonic Commercial Transports Entering Service in the 2030-35 Period", 2007
- [4] International Air Transport Association. "IATA Calls for a Zero Emissions Future", Press Release No.21, 4 June 2007, published in <http://www.iata.org>, cited: 30 May 2011
- [5] Seitz, A., Gologan, C. "Parametric design studies for propulsive fuselage aircraft concepts", *CEAS Aeronautical Journal*, Vol. 6, Issue 1, pp. 69-82, 2015, DOI 10.1007/s13272-014-0130-3
- [6] Bijewitz, J., Seitz, A., Isikveren, A.T., Hornung M. "Multi-disciplinary design investigation of propulsive fuselage aircraft concepts", *Aircraft Engineering and Aerospace Technology*, Vol. 88, Issue 2, pp. 257-267, 2016, DOI: 10.1108/AEAT-02-2015-0053
- [7] Bijewitz, J., Seitz, A., Isikveren, A.T., Hornung M. "Progress in optimizing the propulsive fuselage aircraft concept", AIAA-2016-0767, 54th AIAA Aerospace Sciences Meeting, San Diego, California, 2016
- [8] Isikveren, A.T., Seitz, A., Bijewitz, J., Mirzoyan, A., Isyanov, A., Grenon, R., Atinault, O., Godard, J.L., Stückl, S. "Distributed propulsion and ultra-high by-pass rotor study at aircraft level", *The Aeronautical Journal*, Vol. 119, No. 1221, pp. 1327-1376, 2015, DOI: 10.1017/s0001924000011295
- [9] Welstead, J., Felder, J. "Conceptual design of a single-aisle turboelectric commercial transport with fuselage boundary layer ingestion", AIAA 2016-1027, 54th AIAA Aerospace Sciences Meeting, San Diego, California, 2016
- [10] Stückl, S., van Toor, J., Lobentanzer, H. "VoltAir – the all electric propulsion concept platform – a vision for atmospheric friendly flight", 28th International Congress of the Aeronautical Sciences, Brisbane, Australia, 2012

## A REVIEW OF RECENT AIRCRAFT CONCEPTS EMPLOYING SYNERGISTIC PROPULSION-AIRFRAME INTEGRATION

- [11] Bradley, M., Droney, C. "Subsonic ultra green aircraft research phase II: N+4 advanced concept development", NASA CR-2012-217556, 2012
- [12] Drela, M. "Development of the D8 transport configuration", AIAA-2011-3970, 29th AIAA Applied Aerodynamic Conference, Honolulu, Hawaii, 2011
- [13] Kim, H.D., Felder, J., Tong, M., Berton, J., Haller, B. "Turboelectric distributed propulsion benefits on the N3-X vehicle", *Aircraft Engineering and Aerospace Technology*, Vol. 86, Issue 06, pp. 558-561, 2014, DOI 10.1108/AEAT-04-2014-0037
- [14] Hileman, J.I., Spakovszky, Z., Drela, M., Sargeant, M., Jones, A. "Airframe design for silent fuel-efficient aircraft", *Journal of Aircraft*, Vol. 47, No. 3, pp. 956-969, DOI: 10.2514/1.46545, 2010
- [15] Greitzer, E., *et al.* "N+3 aircraft concept design and trade studies, Final Report Vol. 1", NASA CR-2010-216794/VOL1, 2010
- [16] Tong, M., Jones, S., Haller, W., Handschuh, R. "Engine conceptual design studies for a hybrid wing body aircraft", NASA TM-2009-215680, 2009
- [17] Luongo, C., Masson, P., Nam, T., Mavris, D., Kim, H.D., Brown, G., Waters, M., Hall, D. "Next generation more-electric aircraft: a potential application for HTS superconductors", *IEEE Transactions on Applied Superconductivity*, Vol. 19, No. 3, Part 2, pp. 1055-1068, 2009
- [18] Gibson, A., Hall, D., Waters, M., Schiltgen, B., Foster, T., Keith, J., Masson, P. "The potential and challenge of turboelectric propulsion for subsonic transport aircraft", AIAA 2010-276, 48th AIAA Aerospace Sciences Meeting Including the New Horizons Forum and Aerospace Exposition, Orlando, Florida, 2010
- [19] Brown, G. "Weights and efficiencies of electric components of a turboelectric aircraft propulsion system", AIAA 2011-225, 49th AIAA Aerospace Sciences Meeting including the New Horizons Forum and Aerospace Exposition, Orlando, Florida, 2010
- [20] Schiltgen, B., Gibson, A., Green, M., Freeman, J. "More electric aircraft: "tube and wing" hybrid electric distributed propulsion with superconducting and conventional electric machines", SAE Technical Paper 2013-01-2306, 2013, DOI: 10.4271/2013-01-2306
- [21] Isikveren, A. T., Seitz, A., Vratny, P. C., Pomet, C., Plötner, K., Hornung, M. "Conceptual studies of universally-electric system architectures suitable for transport aircraft", Deutscher Luft- und Raumfahrt-kongress (DLRK), Berlin, 2012
- [22] Vratny, P.C., Forsbach, P., Seitz, A., Hornung M. "Investigation of universally electric propulsion systems for transport aircraft", 29th Congress of the International Council of the Aeronautical Sciences, St. Petersburg, Russia, 7-12 September, 2014
- [23] Seitz, A., Hornung, M. "Pre-concept investigation of hybrid- and full-electric aero propulsion", AVT-230/RSM-033 Specialists Meeting on Advanced Aircraft Propulsion Systems, Rzeszów, Poland, 2015
- [24] Stoll, A., Bevirt, J., Moore, M., Fredericks, W., Borer, N. "Drag reduction through distributed electric propulsion", AIAA-2014-2851, 14th AIAA Aviation Technology, Integration, and Operations Conference, Atlanta, Georgia, 2014
- [25] Stoll, A., Bevirt, J., Pei, P., Stilson, E. "Conceptual design of the Joby S2 electric VTOL PAV", AIAA-2014-2407, 14th AIAA Aviation Technology, Integration, and Operations Conference, Atlanta, Georgia, 2014
- [26] Moore, M. "Personal air vehicles: a rural/regional and intra-urban on-demand transportation system", AIAA 2003-2646, AIAA/ICAS International Air and Space Symposium and Exposition, Dayton, Ohio, 2003
- [27] Moore, M. "NASA personal air transportation technologies" SAE Technical Paper 2006-01-2413, 2006, DOI: 10.4271/2006-01-2413
- [28] Reynolds, K., Nguyen, N., Ting, E., Urnes Sr., J. "Wing shaping concepts using distributed propulsion", *Aircraft Engineering and Aerospace Technology*, Vol. 86, Issue 06, 2014, DOI 10.1108/AEAT-04-2014-0050
- [29] Gerdes, R. "Lift-fan aircraft: lessons learned from XV-5 flight experience", AIAA-93-4838-CP, AIAA International Powered Lift Conference, Santa Clara, California, 1993
- [30] Winborn, B. "ADAM III V/STOL concept", *Journal of Aircraft*, Vol. 7, No. 2, pp. 175-181, 1970, DOI: 10.2514/3.44143
- [31] Ko, A., Leifsson, L., Mason, W., Schetz, J., Grossman, B., Haftka, R. "MDO of a blended-wing-body transport aircraft with distributed propulsion", AIAA 2003-6732, AIAA's 3rd Annual Aviation Technology, Integration, and Operations (ATIO), 2003
- [32] Sehra, A., Whitlow, W. "Propulsion and power for 21st century aviation", *Progress in Aerospace Sciences*, Vol. 40, pp. 199-235, 2004, DOI: 10.1016/j.paerosci.2004.06.003
- [33] Kim, H.D. "Distributed propulsion vehicles", 27th Congress of the International Council of the Aeronautical Sciences, Nice, France, 2010
- [34] Gohardani, A., Doulgeris, G., Singh, R. "Challenges of future aircraft propulsion: A review of distributed propulsion technology and its potential application for the all electric commercial aircraft", *Progress in Aerospace Sciences*, Vol. 47, Issues 1-2, pp. 369-391, 2011, DOI: 10.1016/j.paerosci.2010.09.001
- [35] Gohardani, A. "A synergistic glance at the prospects of distributed propulsion technology and the electric aircraft concept for future unmanned air vehicles and commercial/military aviation", *Progress in Aerospace Sciences*, Vol. 57, pp. 25-70, 2013, DOI: 10.1016/j.paerosci.2012.08.001
- [36] Nalianda, D., Singh, R. "Turbo-electric distributed propulsion – opportunities, benefits and challenges", *Aircraft Engineering and Aerospace Technology*, Vol. 86, Issue 06, 2014, DOI: 10.1108/AEAT-03-2014-0035
- [37] Laskaridis, P. "Application of distributed propulsion concept on different Aircraft configurations", ISABE-2015-20284, 2015
- [38] Rolt, A., Whurr, J. "Distributed propulsion systems to maximize the benefits of boundary layer ingestion", ISABE-2015-20288, 2015
- [39] Hancock, J. "Test of a high efficiency transverse fan", AIAA-80-1243, AIAA/SAE/ASME 16th Joint Propulsion Conference, Hartford, Connecticut, 1980
- [40] Kummer, J., Dang, T. "High-lift propulsive airfoil with integrated crossflow fan", *Journal of Aircraft*, Vol. 43, No. 4, pp. 1059-1068, 2006, DOI: 10.2514/1.17610

- [41] Dang, T., Bushnell, P. "Aerodynamics of cross-flow fans and their application to aircraft propulsion and flow control", *Progress in Aerospace Sciences*, Vol. 45, Issues 1-3, pp. 1-29, 2009, DOI: 10.1016/j.paerosci.2008.10.002
- [42] Gologan, C., Mores, S., Steiner, H.-J., Seitz, A. "Potential of the cross-flow fan for powered-lift regional aircraft applications", AIAA 2009-7098, 9th AIAA Aviation Technology, Integration, and Operations Conference (ATIO), Hilton Head, South Carolina, 2009
- [43] Fredericks, W., Moore, M., Busan, R. "Benefits of hybrid-electric propulsion to achieve 4x increase in cruise efficiency for a VTOL aircraft", AIAA 2013-4324, AIAA Aviation, 2013
- [44] Uranga, A., Drela, M., Greitzer, E., Titchener, N., Lieu, M., Siu, N., Huang, A., Gatlin, G., Hannon, J. "Preliminary experimental assessment of the boundary layer ingestion benefit for the D8 aircraft", AIAA 2014-0906, AIAA 52<sup>nd</sup> Aerospace Sciences Meeting, National Harbor, Maryland, 2014
- [45] e-volo website, <http://www.e-volo.com>, accessed 29.04.2015
- [46] Felder, J., Tong, M., Chu, J. "Sensitivity of mission energy consumption to turboelectric distributed propulsion design assumptions of the N3-X hybrid wing body aircraft", AIAA-2012-3701, 48th AIAA/ASME/SAE/ASEE Joint Propulsion Conference & Exhibit, Atlanta, Georgia, 2012
- [47] distributed Open-rotor AiRcraft (SOAR), [http://cordis.europa.eu/project/rcn/110975\\_en.html](http://cordis.europa.eu/project/rcn/110975_en.html), accessed 16.03.2015
- [48] Stoll, A., Stilson, E., Bewirt, J., Sinha, P. "A multifunctional rotor concept for quiet and efficient VTOL aircraft", AIAA 2013-4374, AIAA Aviation Technology, Integration, and Operations Conference, Los Angeles, California, 2013
- [49] Hall, C., Schwartz, E., Hileman, J. "Assessment of technologies for the silent aircraft initiative", *Journal of Propulsion and Power*, Vol. 25, No. 6, 2009, DOI: 10.2514/1.43079
- [50] Quantum Systems website. <http://www.quantum-systems.com>, accessed 05.05.2015
- [51] Paur, J. "Hexplane: the six-engine airliner-helicopter hybrid", <http://www.wired.com/2012/01/hexplane-oliver-vtol/>, accessed 21.05.2015
- [52] Epstein, A. "Distributed propulsion: new opportunities for an old concept", Final Technical Report 11/1/06 – 10/31/07, Massachusetts Institute of Technology, 2007
- [53] Frota, J. *et al.* "NACRE new aircraft concepts research" Final Activity Report 2005-2010
- [54] Leifsson, L., Ko, A., Mason, W., Schetz, J., Haftka, R., Grossman, B. "Multidisciplinary design optimization for a blended wing body transport aircraft with distributed propulsion", MAD Center Report 2005-05-01, Virginia Polytechnic Institute & State University, 2005
- [55] Bauhaus Luftfahrt e.V. "The CLAIRE Liner", Presentation at ILA Berlin Air Show, 2008
- [56] Warwick, G. "Seeking a fan base", Aviation Week & Space Technology, August 31-September 13, 2015
- [57] Warwick, G. "Vertical commute", Aviation Week & Space Technology, July 20-August 2, 2015
- [58] Antcliff, K. "Silicon valley early adopter CONOPs and market study", 2015 Transformative Vertical Flight Workshop, Moffett Field, California, 2015
- [59] Warwick, G. "Aurora wins Darpa VTOL X-Plane bid with unique hybrid", Aviation Week & Space Technology [online], March 4, 2016
- [60] Joby Aviation website, <http://www.jobyaviation.com>, accessed 29.04.2015
- [61] Kim, H.D., Berton, J., Jones, S. "Low noise cruise efficient short take-off and landing transport vehicle study", NASA TM-2007-214659, 2007
- [62] Ahmad, S. *et al.*, "The Sustinere: a turboelectric distributed propulsion regional jet for 2025", University of Virginia, 2013
- [63] Tactical Robotics website, <http://www.tactical-robotics.com>, accessed 08.03.2016
- [64] Urban Aeronautics website, <http://www.urbaero.com>, accessed 08.03.2016
- [65] Pilczer, D. "Noise reduction assessment and preliminary design implications for a functionally-silent aircraft", Master Thesis, Massachusetts Institute of Technology, 2003
- [66] Airbus Group. "Quadcruiser: an innovative hybrid aircraft concept", product brochure, 2014
- [67] Antoniou, M. "Flying qualities and performance evaluation of the Breguet 941 turbo-prop troop transport", U.S. Army Aviation Test Activity, Report ATA-TR-63-6, 1964
- [68] Lorenz, L., Seitz, A., Kuhn, H., Sizmann, A. "Hybrid power trains for future mobility", Deutscher Luft- und Raumfahrtkongress (DLRK), Stuttgart, Germany, 2013
- [69] Donus, F., Bretschneider, S., Schaber, R., Staudacher S. "The architecture and application of preliminary design systems", GT2011-45614, Proceedings of ASME Turbo Expo 2011, Vancouver, Canada, 2011
- [70] Torenbeek, E. *Advanced Aircraft Design*, John Wiley and Sons, Ltd., West Sussex, 2013
- [71] RFB Fantrainer. FanJet Aviation GmbH website. <http://www.fanjetaviation.com>, accessed 28.04.2016
- [72] Douglas XB-42. Klassiker der Luftfahrt. <http://www.klassiker-der-luftfahrt.de>, accessed 28.04.2016
- [73] Grob GF 200. Deutsches Museum. <http://www.deutsches-museum.de>, accessed 28.04.2016
- [74] LearAvia LearFan 2100. <http://www.aviastar.org>, accessed 28.04.2016
- [75] Schmitz, O., Hornung, M. "Unified applicable propulsion system performance metrics" *Journal of Engineering for Gas Turbines and Power*, Vol. 135, Issue 11, 2013, DOI: 10.1115/1.4025066
- [76] Pornet, C., Kaiser, S., Isikveren, A.T., Hornung, M. "Integrated fuel-battery hybrid for a narrow-body sized transport aircraft", *Aircraft Engineering and Aerospace Technology*, Vol. 86, Issue 6, 2014, DOI: 10.1108/AEAT-05-2014-0062
- [77] Pornet, C., Gologan, C., Vratny, P., Seitz, A., Schmitz, O., Isikveren, A., Hornung, M. "Methodology for sizing and performance assessment of hybrid energy aircraft", *Journal of Aircraft*, Vol. 52, No. 1, 2015, DOI: 10.2514/1.C032716



- [78] Vratny, P., Kaiser, S., Seitz, A., Donnerhack, S. "Performance investigation of cycle-integrated parallel-hybrid turboshafts", GT2016-57539, ASME Turbo Expo 2016: Turbomachinery Technical Conference and Exposition, Seoul, South Korea, 2016
- [79] International Civil Aviation Organization. "Annex 14 to the Convention on International Civil Aviation – Aerodromes, Vol. I", 6th ed., July 2013
- [80] Seitz, A., Schmitz, O., Isikveren, A.T., Hornung, M. „Electrically powered propulsion: comparison and contrast to gas turbines“, Deutscher Luft- und Raumfahrtkongress (DLRK), Berlin, 2012
- [81] Torenbeek, E. *Synthesis of subsonic airplane design*, Kluwer Academic Publishers, Dordrecht/Boston/London, 1982
- [82] Raymer, D. *Aircraft design: a conceptual approach*, 4th ed., AIAA Education Series, American Institute of Aeronautics and Astronautics, Inc., New York, New York, 2006
- [83] Kundu, A. *Aircraft Design*, Cambridge University Press, Cambridge, 2010

### **Contact Author Email Address**

julian.bijewitz@bauhaus-luftfahrt.net

### **Copyright Statement**

The authors confirm that they, and/or their company or organization, hold copyright on all of the original material included in this paper. The authors also confirm that they have obtained permission, from the copyright holder of any third party material included in this paper, to publish it as part of their paper. The authors confirm that they give permission, or have obtained permission from the copyright holder of this paper, for the publication and distribution of this paper as part of the ICAS 2016 proceedings or as individual off-prints from the proceedings.